

**Please cite the Published Version**

Joseph, Ifeoma V, Roncaglia, Giulia, Tosheva, Lubomira and Doyle, Aidan M  (2019) Waste peat ash mineralogy and transformation to microporous zeolites. *Fuel Processing Technology*, 194. ISSN 0378-3820

**DOI:** <https://doi.org/10.1016/j.fuproc.2019.106124>

**Publisher:** Elsevier BV

**Version:** Accepted Version

**Downloaded from:** <https://e-space.mmu.ac.uk/623158/>

**Usage rights:**  [Creative Commons: Attribution-Noncommercial-No Derivative Works 4.0](https://creativecommons.org/licenses/by-nc-nd/4.0/)

**Additional Information:** This is an Author Accepted Manuscript of a paper accepted for publication in *Fuel Processing Technology*, published by and copyright Elsevier.

**Enquiries:**

If you have questions about this document, contact [openresearch@mmu.ac.uk](mailto:openresearch@mmu.ac.uk). Please include the URL of the record in e-space. If you believe that your, or a third party's rights have been compromised through this document please see our Take Down policy (available from <https://www.mmu.ac.uk/library/using-the-library/policies-and-guidelines>)

1                   **Waste peat ash mineralogy and transformation to microporous zeolites**

2                   **Ifeoma V. Joseph, Giulia Roncaglia, Lubomira Tosheva, Aidan M. Doyle\***

3  
4   Department of Natural Sciences, Manchester Metropolitan University, Chester St.,  
5   Manchester, M1 5GD, United Kingdom.

6  
7   \* Corresponding author: [a.m.doyle@mmu.ac.uk](mailto:a.m.doyle@mmu.ac.uk)

8  
9   **Abstract**

10   The combustion of peat fuel for industrial scale power generation and domestic heating  
11   produces toxic ash, most of which is presently buried in landfill. In this study, the mineralogy  
12   of waste peat ash was determined, followed by its successful use as a starting reagent to prepare  
13   zeolites. X-ray diffraction (XRD) confirmed the presence of quartz, anhydrite, calcite, lime,  
14   merwinite and magnetite in peat ash, and that a single extraction step using mineral acid was  
15   sufficient to remove all non-quartz crystal phases. Alkali fusion of the acid-extracted samples  
16   produced GIS-type zeolite. LTA- and FAU-type were also prepared by altering the Si/Al ratio  
17   and extending the ageing time. Experiments confirmed that the LTA- and FAU-type zeolites  
18   were active in the simultaneous adsorption of lead, cadmium, cobalt, zinc and copper from  
19   aqueous solutions, with similar quantities of metals removed to those using a reference zeolite.

20  
21   **Keywords;** Peat ash utilisation; zeolite; pyrolysis; waste management; water purification.

## 26 **1. Introduction**

27 Peat is a carbon based material produced from partially decayed vegetation that builds up over  
28 a duration typically up to approximately 12,000 years [1,2]. The deficiencies of oxygen and  
29 nutrients in waterlogged bogs and fens (peatlands) limit the decay rate of vegetation such that  
30 there is an accumulation of peat over time. These peatlands cover an estimated global area of  
31 4m km<sup>2</sup>, which equates to 2-3% of the total land area, and are found mainly in Russia, North  
32 and South America, Northern Europe and South-East Asia, including lower quantities in  
33 locations such as central Africa [1,2]. Peat is classified as an intermediate fuel i.e. between  
34 biomass and fossil fuel (lignite). Total global consumption is estimated at 17m tons per annum,  
35 over 99% of which is used in Northern Europe for the production of heat and electricity [3].  
36 Ireland is the largest user, consuming 3.8m tons annually from peatlands that cover  
37 approximately 20% of the national land area [4]. Most of this is used in thermal power plants  
38 to generate 8.5% of Ireland's electricity [5,6]. While renewable fuel sources are increasingly  
39 being used as a substitute for peat (at least partially in the short term), the production of  
40 electricity in Ireland using peat based fuel is an established industry with a secure, indigenous  
41 energy source, and will, therefore, continue for the foreseeable future.

42 Peat ash is the main waste product of combustion at thermal power stations, some of which is  
43 disposed of by landfill burial. The alkalinity of peat ash alters the soil quality of the landfill site  
44 such that only alkali tolerant plants can grow during the years immediately after disposal. The  
45 composition of peat ash varies with location but typically contains a mixture of silicon-,  
46 aluminium-, calcium- and iron-containing species, and a range of toxic elements including  
47 arsenic and cadmium [7-10]. While its elemental composition has been well studied, a  
48 definitive characterisation of peat ash mineralogy is lacking in the literature. The few papers  
49 that discuss peat ash infer crystal phases from (a) elemental composition by scanning electron  
50 microscopy/energy-dispersive X-ray spectroscopy (SEM/EDAX) or X-ray fluorescence (XRF)

51 only and/or (b) unseen XRD data; the reader is thus advised to treat such assertions with  
52 caution. For example, quartz, microcline, albite and calcium sulfate were reported to be present  
53 in peat ash samples, although no XRD results were shown [7, 8].

54 The transformation of peat ash to a useful value-added product with industrial applications  
55 would be a significant improvement on the current method of disposal. One such possibility is  
56 to use peat ash to prepare zeolites, which are high surface area aluminosilicates widely used  
57 for water treatment and purification, humidity control, and heterogeneous catalysis [11]. The  
58 combustion of fossil fuels and biomass produces ash residue that contains silicon and  
59 aluminium based minerals in appropriate quantities to those used to prepare aluminosilicate  
60 zeolites. Coal fly ash has been extensively studied as a zeolite synthesis reagent, and a variety  
61 of zeolite architectures were successfully prepared using the alkali fusion method [12-23].  
62 More recently, there are reports showing zeolite preparation using ash from the following  
63 renewable biomass sources: rice husk [24-27] eucalyptus bark residue [28], pulp from paper  
64 industry [29], sawdust and pine bark [30], bamboo [31] and cogon grass [32].

65 We now report the mineralogy of peat ash and its successful transformation to pure zeolite  
66 using a single stage purification step. To our knowledge, this is the first report of zeolite  
67 prepared using peat ash. The zeolites formed removed heavy metals from aqueous solution  
68 with practically similar quantities to those of a reference zeolite.

69

## 70 **2. Materials and Methods**

### 71 **2.1 Materials**

72 Peat ash, from Ireland, was collected and combusted as follows: (a) sample A (lime added),  
73 *Bord na Móna Ltd.*, industrial boiler (b) sample B, air-dried peat sods from county Roscommon,  
74 domestic stove. The following is a list of the materials' source/supplier and purity; hydrochloric  
75 acid (HCl), concentration >37%, Fluka; nitric acid 70% w/w; sodium hydroxide (NaOH)

76 pellets (anhydrous), extra pure, Sigma-Aldrich; sodium aluminate ( $\text{NaAlO}_2$ ), general purpose,  
77 Fischer; sodium silicate solution, general purpose, Merck. Copper(II) nitrate trihydrate  
78  $\text{Cu}(\text{NO}_3)_2 \cdot 3\text{H}_2\text{O}$ , cobalt(II) nitrate hexahydrate  $\text{Co}(\text{NO}_3)_2 \cdot 6\text{H}_2\text{O}$ , lead nitrate  $\text{Pb}(\text{NO}_3)_2$ , zinc  
79 nitrate hexahydrate  $\text{Zn}(\text{NO}_3)_2 \cdot 6\text{H}_2\text{O}$  and cadmium nitrate tetrahydrate  $\text{Cd}(\text{NO}_3)_2 \cdot 4\text{H}_2\text{O}$  were  
80 all 99.99% purity and supplied by Sigma-Aldrich.

81

## 82 **2.2 Zeolite synthesis**

83 The samples were calcined in air at 600 °C (sample A) and 800 °C (sample B) for 4 h to remove  
84 organic matter. Acid extraction was conducted by treating 30 g of calcined peat ash in 500 cm<sup>3</sup>  
85 acid for 5 h as follows: Sample A was stirred in 5 M  $\text{HNO}_3$  at room temperature, and sample  
86 B was refluxed in 5 M  $\text{HCl}$  at 95 °C. The product was recovered by filtration and dried at 80  
87 °C. Unless otherwise stated, 1 part of the acid extracted ash was ground in a mortar and pestle  
88 with 2.4 parts (by mass)  $\text{NaOH}$ , heated at 600 °C in air for 3 h in a furnace, and crushed to  
89 powder form after cooling to ambient temperature. 1 part alkali fused ash was then added to 10  
90 parts water in a polypropylene bottle, stirred at room temperature for 3 days, and  
91 hydrothermally treated at 90 °C for 24 h. Sodium aluminate was added prior to alkali fusion to  
92 give Si/Al ratios (of synthesis reagents) of 5 and 1 to produce GIS and LTA, respectively.  
93 Additional ageing of the Si/Al ratio 1 suspension was done for 4 days at 35 °C to produce FAU.  
94 Products were recovered by filtration and calcined in air at 550 °C for 4 h using a ramp rate of  
95 5 °C min<sup>-1</sup>. A reference FAU zeolite was prepared from a synthesis solution with the molar  
96 composition  $8\text{NaOH} : 0.2\text{Al}_2\text{O}_3 : 1.0\text{SiO}_2 : 200\text{H}_2\text{O}$  [33]. The hydrothermal treatment was  
97 performed at 80 °C for 24 h.

98

## 99 **2.3 Characterisation**

100 XRD was conducted in ambient conditions using a Panalytical X'Pert Powder diffractometer  
101 with Cu K $\alpha$  radiation ( $\lambda = 1.5406 \text{ \AA}$ ). All powder diffraction patterns were recorded from 4 to  
102  $120^\circ 2\theta$  with step size  $0.013^\circ$  and step time 50 s, using an X-ray tube operated at 40 kV and  
103 30 mA with fixed  $\frac{1}{4}^\circ$  anti-scatter slit. A Rigaku NEX-CG (XRF) spectrometer was used for  
104 elemental analysis using the loose powder method under vacuum. Nitrogen  
105 adsorption/desorption measurements were carried out using a Micromeritics ASAP 2020  
106 surface area analyser at  $-196^\circ\text{C}$ . Samples were degassed under vacuum ( $p < 10^{-5}$  mbar) for 5  
107 h at  $200^\circ\text{C}$  prior to analysis. Brunauer–Emmett–Teller (BET) surface areas of the samples  
108 were calculated in the relative pressure range 0.05–0.30. Microscopic images were recorded  
109 using a JEOL JSM-5600LV SEM.

110

## 111 **2.4 Adsorption study**

112  $\text{Cu}(\text{NO}_3)_2 \cdot 3\text{H}_2\text{O}$ ,  $\text{Co}(\text{NO}_3)_2 \cdot 6\text{H}_2\text{O}$ ,  $\text{Pb}(\text{NO}_3)_2$ ,  $\text{Zn}(\text{NO}_3)_2 \cdot 6\text{H}_2\text{O}$  and  $\text{Cd}(\text{NO}_3)_2 \cdot 4\text{H}_2\text{O}$  were  
113 dissolved together in water and diluted to give a solution that was 100 ppm in each of Cu, Co,  
114 Pd, Zn and Cd.  $20 \text{ cm}^3$  of this solution were added to 0.1 g LTA (sample A), stirred at 180 rpm  
115 for 1 h at room temperature and the solid removed by filtration. The concentrations of metals  
116 before and after adsorption were determined using a Thermo Scientific iCAP 6000 Series  
117 inductively coupled plasma-optical emissions spectrometer (ICP-OES).

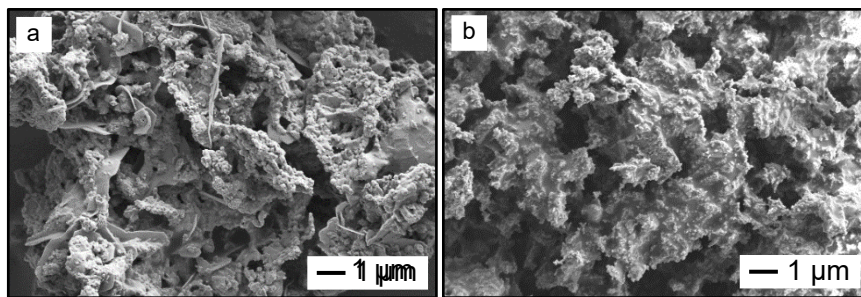
118

## 119 **3. Results and Discussion**

### 120 **3.1 Crystallography and elemental composition**

121 SEM images, Fig. 1, show that both raw and calcined peat ash lack any regular morphology,  
122 which is in contrast to the spherically shaped particles routinely observed for coal fly ash [12].  
123 Results also showed that calcination did not cause an observable transformation in particle  
124 morphology. Phase identification, performed by matching the XRD peak positions in Fig. 2

125 against the Crystallography Open Database, confirms that the major phases detected for sample  
 126 A are anhydrite ( $\text{CaSO}_4$ ), quartz ( $\text{SiO}_2$ ), calcite ( $\text{CaCO}_3$ ), lime ( $\text{CaO}$ ) and merwinite  
 127 ( $\text{Ca}_3\text{Mg}(\text{SiO}_4)_2$ ). Sample B contains anhydrite, quartz and magnetite ( $\text{Fe}_3\text{O}_4$ ). A quantitative  
 128 elemental analysis using XRF, Table 1, shows the 10 most concentrated elements present (for  
 129 sample A) and confirms that the major ‘impurities’ (in terms of zeolite synthesis) are Ca and  
 130 Fe based species. The major element present in Sample A is Ca at 53.9 wt% (as oxide) in  
 131 agreement with the XRD analysis (Fig. 2). Sample B contains 21.2 wt% CaO and 22.0 wt%  
 132  $\text{Fe}_2\text{O}_3$ . The greater quantity of CaO in sample A is due to the addition of lime to commercial  
 133 peat to reduce  $\text{SO}_x$  emissions, which may have reacted to produce anhydrite. It is interesting  
 134 then that sample B, which has not been treated with lime, also contains anhydrite.



140 Fig. 1. Typical SEM images of peat ash: (a) raw and (b) calcined.

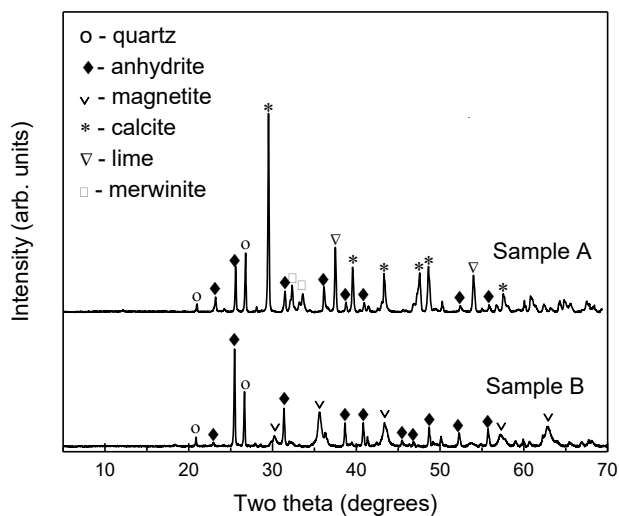


Fig. 2. XRD powder patterns of calcined peat ash.

143

144 It is not possible to make a meaningful comparison of the XRD results presented here with  
145 published data on peat ash mineralogy, as such reports contain insufficient results [7,8].  
146 However, all such studies confirm that the main elements present in peat ash are Ca, Fe, Si and  
147 Al, which correlates well with our XRD and XRF results.

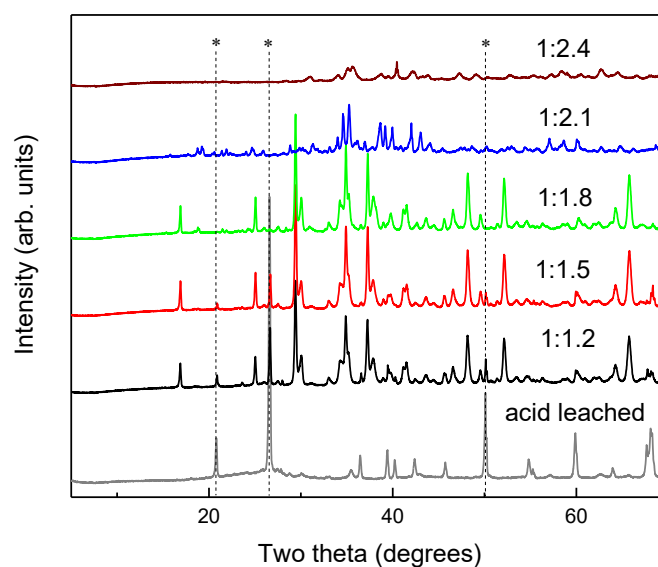
148

149 Table 1: XRF elemental composition of peat ash in wt% following calcination and acid extraction.

	<b>A</b>		<b>B</b>	
	<b>Calcined</b>	<b>Acid extracted</b>	<b>Calcined</b>	<b>Acid extracted</b>
CaO	53.9	0.81	21.2	0.77
SiO <sub>2</sub>	9.47	71.4	12.7	76.9
SO <sub>3</sub>	7.32	0.58	22.4	0.26
Fe <sub>2</sub> O <sub>3</sub>	4.81	1.29	22.0	0.61
MgO	2.20	0.12	10.4	0.35
Al <sub>2</sub> O <sub>3</sub>	1.63	2.55	6.58	3.77
MnO	0.35	0.03	0.30	0.02
P <sub>2</sub> O <sub>5</sub>	0.26	0.05	1.87	0.05
K <sub>2</sub> O	0.19	0.97	0.97	1.12
TiO <sub>2</sub>	0.15	0.50	0.45	0.90

150

151 Dissolution by acid extraction considerably reduced the quantities of Ca and Fe in both  
152 samples. The Si/Al ratios of acid extracted peat ashes are 28.0 for sample A and 20.4 for sample  
153 B. XRD patterns confirm that acid extraction removes all detectable non-quartz crystalline  
154 phases, Fig. 3. The majority of zeolite preparations using coal ash do not remove impurities by  
155 acid extraction, so it is not surprising that a greater ratio of NaOH to ash is required for the peat  
156 ash samples explored here to achieve full quartz decomposition due to the higher quantity of  
157 quartz [12]. Fig. 3 shows that the mass ratio of 1.2:1 NaOH to ash (chosen as a starting point  
158 based on reference [22]) was insufficient but that higher ratios removed quartz completely; a  
159 mass ratio of 2.4:1 was used in all further preparations. The other peaks in Fig. 3 confirm the  
160 presence of silicates and aluminosilicates, as reported in the literature [34].



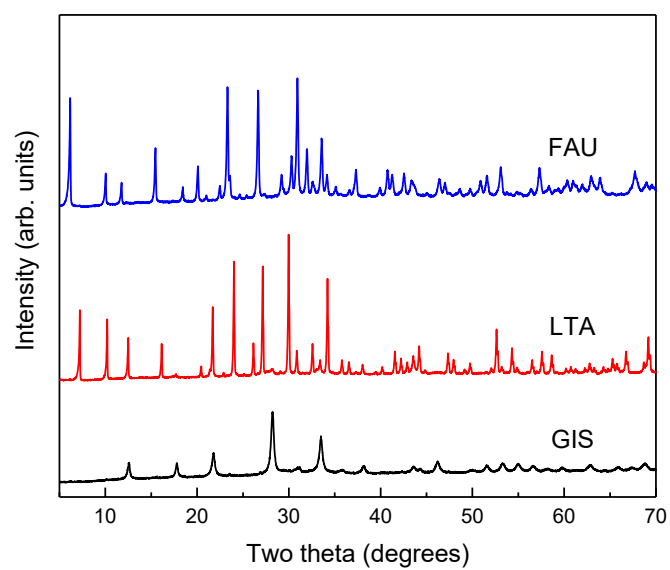
161

162 Fig. 3. XRD patterns of sample A after acid leaching and the acid-leached sample after alkali fusion at  
 163 600 °C using different sample:NaOH mass ratios as indicated on the figure; the asterisks indicate  
 164 quartz peaks.

165

### 166 3.2 Zeolite formation

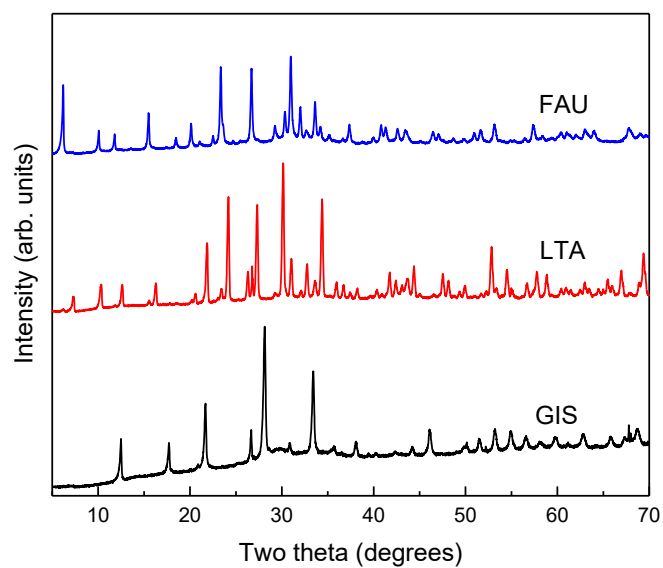
167 The XRD patterns in Figs. 4 and 5 confirm that peat ash was transformed to zeolite frameworks  
 168 GIS, LTA and FAU through changes in the synthesis parameters viz. addition of sodium  
 169 aluminate for LTA, and extended ageing time for FAU. Non-zeolitic crystalline phases were  
 170 not observed by XRD in any detectable quantities. The effect of altering the Si/Al ratio by  
 171 adding external silica was found to alter the crystal phase produced in a study of the  
 172 crystallisation mechanism of zeolite from coal fly ash, where FAU was not formed until the  
 173 Si/Al ratio was reduced to approximately 1.5 [35]. SEM images, Fig. 6, show the morphology  
 174 of GIS, the characteristic cubic ca. 1  $\mu\text{m}$  sized particles of LTA and the sub-micron  
 175 agglomerated FAU particle morphology, providing further evidence of the presence of these  
 176 phases. The Si/Al ratios are shown in Table 2: the Si/Al ratios of FAU are 1.32 and 1.35, so  
 177 these samples are zeolite X. The highest BET surface areas were recorded for the FAU  
 178 structures, which were calculated to be 486 and 319  $\text{m}^2 \text{g}^{-1}$ .



179

180

Fig. 4 XRD patterns of zeolites prepared using sample A.



181

182

Fig. 5 XRD patterns of zeolites prepared using sample B.

183

184

185

186

187

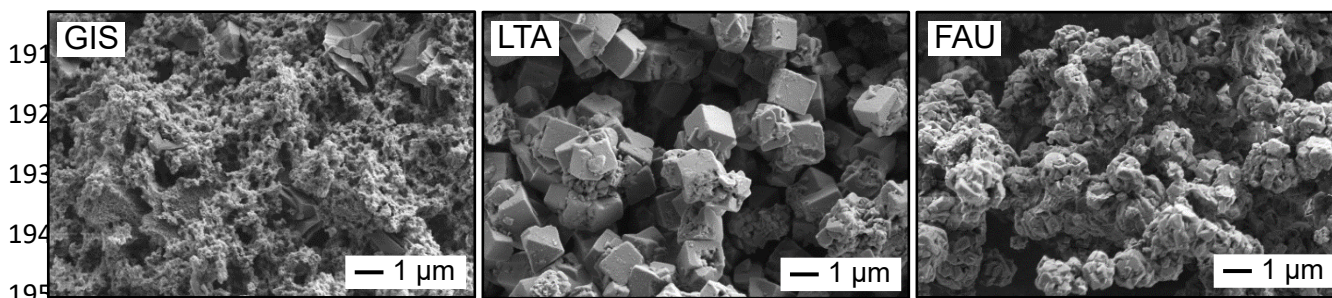
188

Table 2: BET surface areas and Si/Al elemental ratios.

	Surface area ( $\text{m}^2 \text{g}^{-1}$ )		Si/Al	
	A	B	A	B
Raw	24	25	4.04	1.55
Calcined	6	22	4.94	1.64
FAU	486	319	1.32	1.35
LTA	84	55	1.41	1.35
GIS	77	104	2.83	2.83

189

190



196 Fig. 6. Typical SEM images of different zeolites types prepared from peat ash.

197

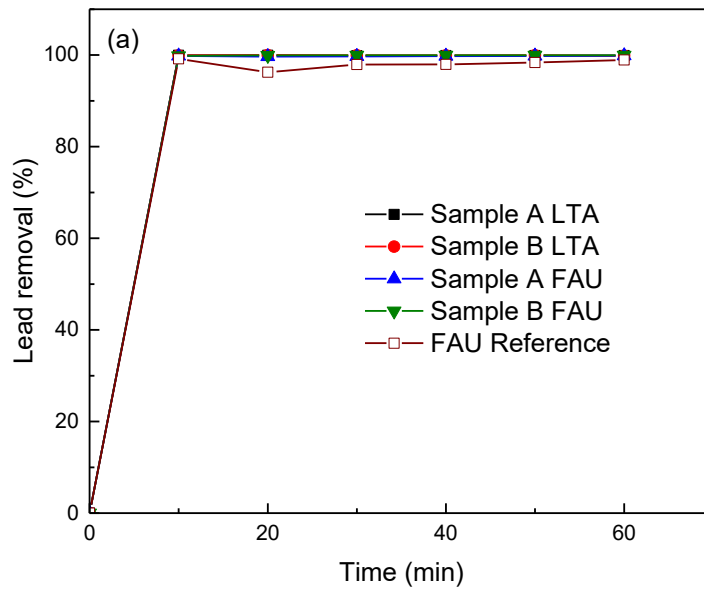
198 The characteristics of zeolites prepared from peat ash also compare well with analogous studies  
 199 using fly ash. For example, the highest surface area reported by Tosheva et al. for FAU  
 200 prepared from fly ash was  $441 \text{ m}^2 \text{g}^{-1}$ , relative to  $486 \text{ m}^2 \text{g}^{-1}$  for that prepared here [23]. The  
 201 classification of coal is based on the relative amounts of organic and inorganic materials, age,  
 202 and quantity of heat energy that can be produced. Most reports in the literature describing coal  
 203 ash to zeolite conversions are for sub-bituminous (up to 45% carbon) bituminous (86%) and  
 204 anthracitic (97%) coal types. Lignite has lower carbon content than sub-bituminous coal and,  
 205 because it is formed over time from compressed peat, which has carbon content less than 40-  
 206 55%, seems the most appropriate comparison to the results presented here [1-3]. Kunecki et al.  
 207 used lignite, containing quartz, anhydrite and gehlenite, to prepare zeolite [36]. Both LTA and  
 208 FAU frameworks were prepared by varying experimental conditions, but not in pure form. The  
 209 highest BET surface area for FAU was  $256 \text{ m}^2 \text{g}^{-1}$ , which was significantly lower than the FAU

210 from either sample in this study, 486 and 319 m<sup>2</sup> g<sup>-1</sup>. The increased crystal purity and surface  
211 area for zeolite prepared using peat ash is tentatively attributed to the removal of impurities in  
212 the starting material by acid extraction. Anhydrite is highly soluble in aqueous solution and its  
213 presence during zeolite crystallisation, as in the case of lignite to zeolite, reduces the solubility  
214 of silicates and aluminosilicates, which will negatively impact both the formation of zeolite  
215 nuclei and the subsequent dissolution and crystallisation of zeolite during hydrothermal  
216 treatment. Furthermore, ions in solution are known to interact with zeolite frameworks during  
217 crystallisation, so the Ca<sup>2+</sup> and SO<sub>4</sub><sup>2-</sup> ions from anhydrite may have a negative effect on the  
218 formation of zeolite [37].

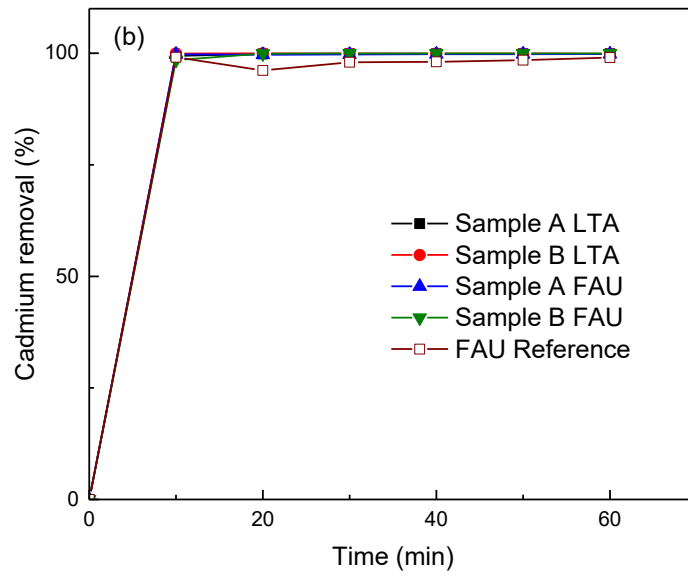
219

### 220 **3.3 Adsorption study**

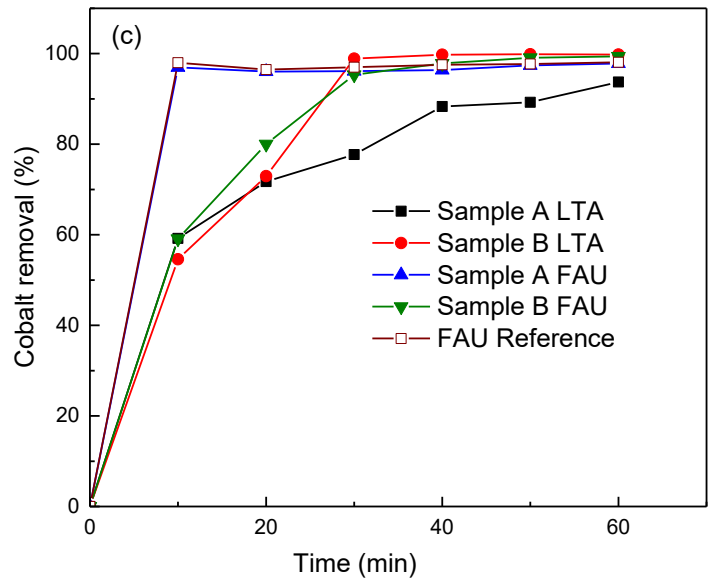
221 The prepared zeolites were tested as adsorbents in the removal of heavy metals lead, cadmium,  
222 cobalt, zinc and copper from aqueous solution; these metals were chosen on the basis of their  
223 toxicity and presence in wastewater streams [38]. The results, Fig. 7, showed that all zeolites  
224 actively removed the range of metals between 10 and 60 minutes, in which the quantities of  
225 lead, cadmium, zinc and copper adsorbed using peat ash prepared zeolites were slightly higher  
226 than those measured for the FAU- reference. In the case of cobalt, adsorption was higher using  
227 FAU-type zeolites than LTA-, while the most active adsorbent was that prepared from sample  
228 A, which showed near identical properties to that of the reference zeolite. A more in-depth  
229 study of metals adsorption on zeolites viz. influence of concentration, temperature, and kinetics  
230 is currently underway and will be published as a follow up to this paper. While the focus of  
231 this paper is the preparation of pure zeolite from peat ash, the adsorption results are included  
232 to validate the efficacy of such materials in real applications.



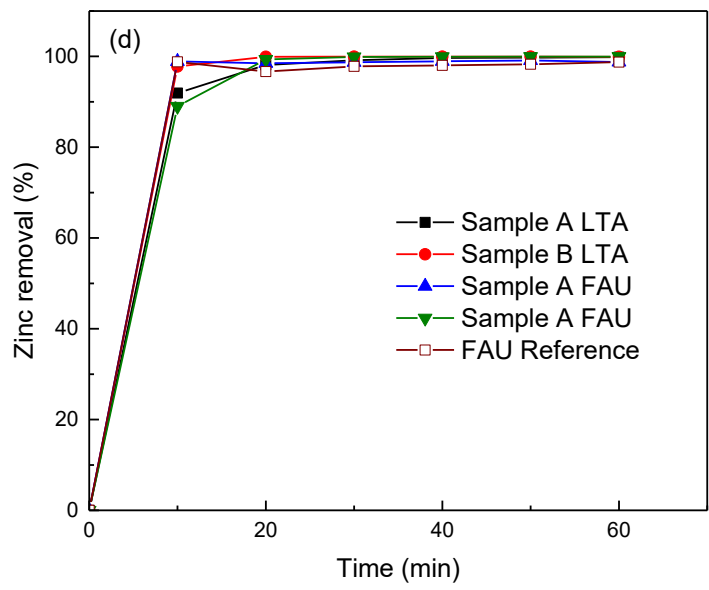
233



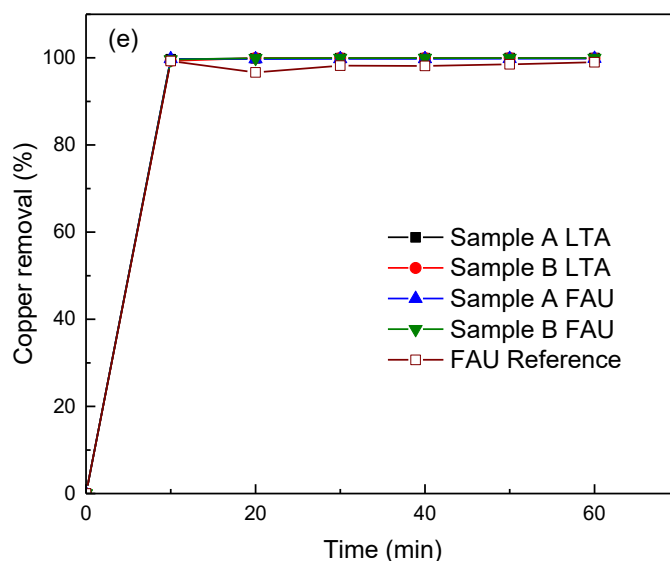
234



235



236



237

238 Fig. 7. Metal removal (as % of original concentration) of (a) lead (b) cadmium (c) cobalt (d) zinc and  
 239 (e) copper on LTA- and FAU-type zeolites prepared from peat ash and an FAU- reference.

240

#### 241 4. Conclusions

242 Zeolites were successfully prepared from peat ash using a combination of acid leaching, alkali  
 243 fusion and hydrothermal treatment. The framework structure was systematically varied such  
 244 that crystal phases of GIS, LTA and FAU-type zeolites were each prepared. The prepared  
 245 zeolites were active in the removal of a range of metals from aqueous solution.

246

#### 247 Acknowledgments:

248 The authors thank; Patrick Bowens, Co. Roscommon, and Imelda Egan and Colman Hynes,  
 249 Bord na Móna, for supplying peat ash; Dr Paul Bolger, University College Cork, for arranging  
 250 the link with Bord na Móna. Ifeoma V Joseph is grateful to the Schlumberger Foundation for  
 251 funding a PhD studentship; Giulia Roncaglia is grateful to Erasmus+ and Manchester  
 252 Metropolitan University for financial assistance.

253

254

255 **References**

- 256 1. F. Parish, A.A. Sirin, D. Charman, H. Joosten, T. Minayeva, M. Silvius, Assessment on  
257 Peatlands, Biodiversity and Climate Change: Executive Summary. Global Environmental  
258 Centre, Malaysia and Wetlands International, Wageningen, The Netherlands, 2007.
- 259 2. E. Lappalainen, Global Peat Resources, The International Peat Society, Finland 1996.
- 260 3. World Energy Council Report, World Energy Resources 2013 Survey: Peat.
- 261 4. Department of Agriculture, Food and the Marine Ireland, Rural Development Programme  
262 2014a.
- 263 5. Sustainable Energy Authority of Ireland 2017 Report, Energy in Ireland 1990-2016.
- 264 6. Eirgrid Group, All-Island Generation Capacity Statement 2017-2026.
- 265 7. J. Fagerström, I.-L. Näzelius, C. Gilbe, D. Boström, M. Öhman, C. Boman, Influence of peat  
266 ash composition on particle emissions and slag formation in biomass grate co-combustion,  
267 Energy Fuels 28 (2014) 3403-3411. <https://dx.doi.org/10.1021/ef4023543>.
- 268 8. L. Pommer, M. Öhman, D. Boström, J. Burvall, R. Backman, I. Olofsson, A. Nordin,  
269 Mechanisms behind the positive effects on bed agglomeration and deposit formation  
270 combusting forest residue with peat additives in fluidized beds, Energy Fuels 23 (2009) 4245-  
271 4253. <https://doi.org/10.1021/ef900146e>.
- 272 9. B-M. Steenari, O. Lindqvist, Fly ash characteristics in co-combustion of wood with coal, oil  
273 or peat, Fuel 78 (1999) 479-488. [https://doi.org/10.1016/S0016-2361\(98\)00177-X](https://doi.org/10.1016/S0016-2361(98)00177-X).
- 274 10. S.V. Vassilev, D. Baxter, L.K. Andersen, C.G. Vassileva, An overview of the composition  
275 and application of biomass ash. Part 1. Phase–mineral and chemical composition and  
276 classification, Fuel 10 (2013) 40-76. <https://doi.org/10.1016/j.fuel.2012.09.041>.
- 277 11. J. Weitkamp, Zeolites and catalysis, Solid State Ionics 131 (2000) 175-188.  
278 [https://doi.org/10.1016/S0167-2738\(00\)00632-9](https://doi.org/10.1016/S0167-2738(00)00632-9).
- 279 12. C. Belviso, State-of-the-art applications of fly ash from coal and biomass: A focus on  
280 zeolite synthesis processes and issues, Prog. Energy Combust. Sci. 65 (2018) 109-135.  
281 <https://doi.org/10.1016/j.pecs.2017.10.004>.
- 282 13. X. Querol, N. Moreno, J.C. Umaña, A. Alastuey, E. Hernández, A. López-Soler, F. Plana,  
283 Synthesis of zeolites from coal fly ash: an overview. Int. J. Coal Geol. 50 (2002) 413-423.  
284 [https://doi.org/10.1016/S0166-5162\(02\)00124-6](https://doi.org/10.1016/S0166-5162(02)00124-6).
- 285 14. X. Querol, J.C. Umaña, F. Plana, A. Alastuey, A. López-Soler, A. Medinaceli, A. Valero,  
286 M.J. Domingo, E. Garcia-Rojo. Synthesis of Na zeolites from fly ash in a pilot plant  
287 scale. Examples of potential environmental applications, Fuel 80 (2001) 857-865.

- 288 15. N. Murayama H. Yamamoto J. Shibata, Mechanism of zeolite synthesis from coal fly ash  
289 by alkali hydrothermal reaction. *Int. J. Miner. Process.* 64 (2002) 1-17.  
290 [https://doi.org/10.1016/S0301-7516\(01\)00046-1](https://doi.org/10.1016/S0301-7516(01)00046-1).
- 291 16. H. Tanaka, S. Matsumura, R. Hino, Formation process of Na-X zeolites from coal fly ash.  
292 *J. Mater. Sci.* 39 (2004) 1677-1682. <https://doi.org/10.1023/B:JMISC.0000016169.85449.86>.
- 293 17. T.T. Walek, F. Saito, Q. Zhang, The effect of low solid/liquid ratio on hydrothermal  
294 synthesis of zeolites from fly ash. *Fuel* 87 (2008) 3194-3199.  
295 <https://doi.org/10.1016/j.fuel.2008.06.006>.
- 296 18. H. Tanaka, A. Fujii. Effect of stirring on the dissolution of coal fly ash and synthesis of  
297 pure-form Na-A and -X zeolites by two-step process, *Adv. Powder Technol.* 20 (2009) 473-  
298 479. <https://10.1016/j.appt.2009.05.004>
- 299 19. M. Gross-Lorgouilloux, P. Gaultet, M. Soulard, J. Patarin, E. Moleiro, I. Saude, Conversion  
300 of coal fly ashes into faujasite under soft temperature and pressure conditions. Mechanisms of  
301 crystallisation, *Microporous Mesoporous Mater.* 131 (2010) 407-417.  
302 <https://doi.org/10.1016/j.micromeso.2010.01.022>.
- 303 20. N. Shigemoto, H. Hayashi, K. Miyaura, Selective formation of Na-X zeolite from coal fly  
304 ash by fusion with sodium hydroxide prior to hydrothermal reaction, *J. Mater. Sci.* 28 (1992)  
305 4781-4786. <https://doi.org/10.1007/BF00414272>.
- 306 21. H.-L. Chang, W.-H. Shih, A general method for the conversion of fly ash into zeolites as  
307 ion exchangers for cesium, *Ind. Eng. Chem. Res.* 37 (1998) 71-78. <https://10.1021/ie970362o>.
- 308 22. A. Molina, C. Poole, A comparative study using two methods to produce zeolites from fly  
309 ash, *Miner. Eng.* 17 (2004) 167-173. <https://doi.org/10.1016/j.mineng.2003.10.025>.
- 310 23. L. Tosheva, A. Brockbank, B. Mihailova, J. Sutula, J. Ludwig, H. Potgieter, J. Verran,  
311 Micron- and nanosized FAU-type zeolites from fly ash for antibacterial applications, *J. Mater.*  
312 *Chem.* 22 (2012) 16897-16905. <https://10.1039/C2JM33180B>.
- 313 24. D. Prasetyoko, Z. Ramli, S. Endud, H. Hamdan, B. Sulikowski, Conversion of rice husk  
314 ash to zeolite beta, *Waste Management*, 26 (2006) 1173-1179.  
315 <https://doi.org/10.1016/j.wasman.2005.09.009>.
- 316 25. R.K. Vempati, R. Borade, R.S. Hegde, S. Komarneni, Template free ZSM-5 from siliceous  
317 rice hull ash with varying C contents, *Microporous Mesoporous Mater.* 93 (2006) 134-140.  
318 <https://doi.org/10.1016/j.micromeso.2006.02.008>.
- 319 26. E.-P. Ng, H. Awala, K.-H. Tan, F. Adam, R.d Retoux, S. Mintova, EMT-type zeolite  
320 nanocrystals synthesized from rice husk, *Microporous Mesoporous Mater.* 204 (2015) 204-  
321 209. <https://doi.org/10.1016/j.micromeso.2014.11.017>.

322 27. Jia-Tian Wong, Eng-Poh Ng, Farook Adam, Microscopic investigation of nanocrystalline  
323 zeolite L synthesized from rice husk ash, *J. Am. Ceram. Soc.* 95 (2012) 805–808.  
324 <https://doi.org/10.1111/j.1551-2916.2011.04995.x>.

325 28. I. Jiménez, G. Pérez, A. Guerrero, B. Ruiz, Mineral phases synthesized by hydrothermal  
326 treatment from biomass ashes, *Int. J. Miner. Process.* 158 (2017) 8-12.  
327 <https://doi.org/10.1016/j.minpro.2016.11.002>.

328 29. S. Vichaphund, D. Aht-Ong, V. Sricharoenchaikul, D. Atong, Characteristic of fly ash  
329 derived-zeolite and its catalytic performance for fast pyrolysis of *Jatropha* waste, *Environ.*  
330 *Technol.* 35 (2014) 2254-61. <https://doi.org/10.1080/09593330.2014.900118>.

331 30. T. Fukasawa, A. Horigome, T. Tsu, A.D. Karisma, N. Maeda, A.-N. Huang, K. Fukui,  
332 Utilization of incineration fly ash from biomass power plants for zeolite synthesis from coal  
333 fly ash by hydrothermal treatment, *Fuel Process. Technol.* 167 (2017) 92–98.  
334 <https://doi.org/10.1016/j.fuproc.2017.06.023>.

335 31. E.-P. Ng, J.-H. Chow, R.R. Mukti, O. Muraza, T.C. Ling, K.-L. Wong, Hydrothermal  
336 synthesis of zeolite A from bamboo leaf biomass and its catalytic activity in cyanoethylation  
337 of methanol under autogenic pressure and air conditions, *Mater. Chem. Phys.* 201 (2017) 78-  
338 85. <https://doi.org/10.1016/j.matchemphys.2017.08.044>.

339 32. K. Bunmai, N. Osakoo, K. Deekamwong, W. Rongchapo, C. Keawkumay, N. Chanlek, S.  
340 Prayoonpokarach, J. Wittayakun, Extraction of silica from cogon grass and utilization for  
341 synthesis of zeolite NaY by conventional and microwave-assisted hydrothermal methods, *J.*  
342 *Taiwan Inst. Chem. E.* 83 (2018) 152–158. <https://doi.org/10.1016/j.jtice.2017.11.024>.

343 33. V. P. Valtchev, K. N. Bozhilov, Transmission electron microscopy study of the formation  
344 of FAU-type zeolite at room temperature, *J. Phys. Chem. B* 108 (2004) 15587-15598.  
345 <https://pubs.acs.org/doi/abs/10.1021/jp048341c>.

346 34. A.M. Doyle, Z.T. Alismaeel, T.M. Albayati, A.S. Abbas, High purity FAU-type zeolite  
347 catalysts from shale rock for biodiesel production, *Fuel* 199 (2017) 394-402.  
348 <https://doi.org/10.1016/j.fuel.2017.02.098>.

349 35. M. Gross-Lorgouilloux, P. Caullet, M. Soulard, J. Patarin, E. Moleiro, I. Saude, Conversion  
350 of coal fly ashes into faujasite under soft temperature and pressure conditions. Mechanisms of  
351 crystallisation, *Microporous and Mesoporous Materials* 131 (2010) 407–417.  
352 <https://doi.org/10.1016/j.micromeso.2010.01.022>.

353

- 354 36. P. Kunecki, R. Panek, M. Wdowin, W. Franus, Synthesis of faujasite (FAU) and  
355 tschernichite (LTA) type zeolites as a potential direction of the development of lime Class C  
356 fly ash, *Int. J. Miner. Process.* 166 (2017) 69-78. <https://doi.org/10.1016/j.minpro.2017.07.007>.
- 357 37. R.M. Shayib, N.C. George, R. Seshadri, A.W. Burton, S.I. Zones, B. F. Chmelka, Structure-  
358 directing roles and interactions of fluoride and organocations with siliceous zeolite  
359 frameworks, *J. Am. Chem. Soc.* 133 (2011) 18728–18741. <https://10.1021/ja205164u>.
- 360 38. F. Fenglian, Q. Wang, Removal of heavy metal ions from wastewaters: A review, *J.*  
361 *Environ. Manage.* 92 (2011) 407-418. <https://doi.org/10.1016/j.jenvman.2010.11.011>.